Arabidopsis ABCG14 protein controls the acropetal translocation of root-synthesized cytokinins

Kewei Zhang[1,†], Ondrej Novak[2], Zhaoyang Wei[1], Mingyue Gou[1], Xuebin Zhang[1], Yong Yu[3], Huijun Yang[1], Yuanheng Cai[1], Miroslav Strnad[2,4] & Chang-Jun Liu[1]

Cytokinins are a major group of phytohormones regulating plant growth, development and stress responses. However, in contrast to the well-defined polar transport of auxins, the molecular basis of cytokinin transport is poorly understood. Here we show that an ATP-binding cassette transporter in *Arabidopsis*, AtABCG14, is essential for the acropetal (root to shoot) translocation of the root-synthesized cytokinins. *AtABCG14* is expressed primarily in the pericycle and stelar cells of roots. Knocking out *AtABCG14* strongly impairs the translocation of *trans*-zeatin (*t*Z)-type cytokinins from roots to shoots, thereby affecting the plant's growth and development. AtABCG14 localizes to the plasma membrane of transformed cells. *In planta* feeding of C^{14} or C^{13}-labelled *t*Z suggests that it acts as an efflux pump and its presence in the cells directly correlates with the transport of the fed cytokinin. Therefore, AtABCG14 is a transporter likely involved in the long-distance translocation of cytokinins *in planta*.

[1] Biosciences Department, Brookhaven National Laboratory, Upton, New York 11973, USA. [2] Laboratory of Growth Regulators, Faculty of Science, Palacký University & Institute of Experimental Botany AS CR, Olomouc CZ-78371, Czech Republic. [3] Department of Biological Sciences, St. John's University, Queens, New York 11439, USA. [4] Centre of the Region Haná for Biotechnological and Agricultural Research, Palacký University, CZ-783 71 Olomouc, Czech Republic. † Present address: College of Chemistry and Life Sciences, Zhejiang Normal University, Jinhua, Zhejiang 321004, China. Correspondence and requests for materials should be addressed to C.-J.L. (email: cliu@bnl.gov).

   1

Cytokinins are a heterogeneous class of N[6]-substituted adenine derivatives with either an isoprene-derived or an aromatic side chain[1–3]. Since their discovery in the 1950s as key promoters of cell division in plants, a plethora of biological functions have been attributed to these signalling molecules, encompassing the regulation of cell division and differentiation[4], chloroplast development[5], leaf senescence[5,6], root- and shoot-apical dominance[7], nutrient balances and stress responses[8]. Plants respond to cytokinins through a two-component signalling pathway: cytokinin binding to histidine-kinase receptors induces a phosphorelay that activates two types of response regulators (RRs), and consequently triggers the signal responses[9].

Isoprenoid cytokinins, including trans-zeatin (tZ), dihydrozeatin (DHZ), cis-zeatin (cZ) and isopentenyladenine (iP), are the most abundant species in higher plants[1]. Chemical profiling of xylem and phloem sap, and reciprocal grafting of roots and shoots of cytokinin-deficient mutants revealed that tZ-type cytokinins are mainly synthesized in roots, and iP-type cytokinins mainly in shoots. They then, respectively, move acropetally through the xylem and basipetally or systemically through the phloem, and are distributed to the action sites[4,10]. Therefore, cytokinins act as both local and long-distance signals in regulating cell division and differentiation. Some in vitro evidence indicates that two types of selective transporter systems may be involved in translocating cytokinin. Members of the Arabidopsis purine permease family, AtPUP1 and PUP2, appear to mediate the import of adenines and nucleobase cytokinins[11,12], while equilibrative nucleoside transporters (ENTs) of both rice and Arabidopsis might mediate the transport of adenosine and other nucleosides, including iP riboside[13,14]. However, definitive proof of the involvement of both types of transporters in cytokinin translocation in planta is lacking[9,15].

ATP-binding cassette (ABC) transporters comprise one of the largest families of transport proteins, catalysing the export and import of numerous metabolites in organisms ranging from bacteria to humans[16]. The Arabidopsis genome contains more than 120 ABC transporter genes[17], most of which encode membrane-bound proteins[17]. ABC subfamily G (ABCG) includes 28 members of the white–brown complex half transporters, and 15 pleiotropic drug resistance full transporters[16]. Several members of this subfamily have demonstrated responsibility for exporting wax and cutin used in the formation of cuticle in aerial organs[18], for conveying abscisic acid across the plasma membrane in leaf guard cells[19] and for exporting auxinic compounds, including indole-3-butyric acid[20]. Seemingly, the ABCG subfamily proteins participate in various biological processes. Nevertheless, although growing numbers of this subfamily of proteins have been characterized, the biological and biochemical functions of many of ABCG proteins remain undetermined.

In this study, using a reverse genetics approach to systematically characterize the ABCG proteins, we note that the disruption of AtABCG14 in null mutant lines severely impairs the long-distance translocation and distribution of the root-synthesized tZ-type cytokinin species, which subsequently causes substantial morphological alterations in the growth and development of roots and shoots; furthermore, our in planta feeding and detached leaf assay using a radiolabelled tracer demonstrates an efflux pump activity of AtABCG14 to the fed cytokinin. Therefore, AtABCG14 is a transporter likely involved in the control of acropetal long-distance translocation of tZ-type cytokinins in planta.

Results

Disruption of AtABCG14 causes cytokinin-deficient phenotypes.
Conducting in silico gene expression analysis on a set of Arabidopsis ABCG transporters with unknown function, we found that one of the subfamily members, AtABCG14, is highly expressed in the vascular tissues of roots. To examine this gene's function, we obtained two T-DNA insertion mutant alleles, SK_15917 and SK_15918, from Arabidopsis Biological Research Center. By genotyping and reverse transcriptional polymerase chain reaction (RT–PCR) analysis, we verified that both lines with T-DNA insertions in the second exon of the gene are null mutants; we designated them as atabcg14-1 and atabcg14-2 (Supplementary Fig. 1). When grown under normal conditions, both mutant lines exhibited weaker growth, smaller inflorescences and rosettes, slenderer stems and shorter primary roots than their wild-type counterparts (Fig. 1a–e and Supplementary Fig. 2). These morphological alterations are reminiscent of the symptoms of cytokinin deficiency in the cytokinin receptor mutant lines ahk2/ahk3 (ref. 21) and in plants overexpressing Arabidopsis CYTOKININ OXIDASE (AtCKX)[22], implying that both mutants might have defective cytokinin signalling pathways or responses. Transformation with a genomic DNA sequence comprising the native AtABCG14 promoter, exons and introns completely restored wild-type morphology in these mutant lines (Supplementary Fig. 3), verifying that AtABCG14 deficiency is the cause of the observed phenotypic deviations.

Atabcg14 mutant seedlings exhibited severe retardation of primary root elongation (Fig. 1e and Supplementary Fig. 4a,b). This phenotype is also consistent with perturbation of cytokinin status, as increase in cytokinin levels normally inhibit root growth and reduce the size of root meristems[22–24]. Thus, we speculated that disrupting AtABCG14 may impair root meristem activity. To test this hypothesis, we employed the CYCB1;1::uidA expression cassette, a widely used mitosis reporter[22,25], to monitor meristem activities in the primary roots of Arabidopsis. When the atabcg14-1 mutant was crossed with a CYCB1;1::uidA transgenic line, β-glucuronidase (GUS) activity was much weaker in the proximal root meristem of homozygous progeny harbouring the CYCB1;1::uidA transgene in an atabcg14-1 mutant background than in CYCB1;1::uidA-expressing progeny with a wild-type background (Supplementary Fig. 4c). These findings confirm that disrupting AtABCG14 deleteriously affects root meristem activity, possibly by disturbing the concentrations or distribution of root cytokinins.

Further, we monitored the responses of root elongation of atabcg14 plants to phytohormones and hormone precursors at various concentrations, including the ethylene precursor 1-aminocyclopropane-1-carboxylic acid (ACC), the auxin 1-naphthaleneacetic acid (NAA) and the cytokinins 6-benzyladenine (BA) and tZ. Exogenously applying these substances to vertically growing seedlings generally inhibited root elongation in a dose-dependent manner (Supplementary Fig. 5). However, root elongation was distinctly less sensitive to BA and tZ treatments in atabcg14 mutants than in wild-type plants. In sharp contrast, responses of the mutant and wild-type plants to exposure to auxin and ACC were indistinguishable (Supplementary Fig. 5). These data further imply that in mutant roots there may be a change in endogenous cytokinin homeostasis or cytokinin-related signalling perception or response.

Consistent with having slender inflorescence stems, the average number of vascular bundles was reduced considerably in the atabcg14 mutant lines, from 8 ± 0.63 (mean $\pm$ s.d., $n = 6$) in wild-type plants to about 5.3 ± 0.52 (mean $\pm$ s.d., $n = 6$) (Fig. 1f–h). This affords us anatomical evidence of cytokinin perturbation in the mutant lines, because, as well as regulating root meristems, cytokinins are key regulators of shoot meristem activity, but in an opposite manner[22,26]. Cytokinin deficiencies reportedly diminish the activities of vegetative and floral shoot meristems, including cambium-mediated secondary growth[4,22,26]. Furthermore, the
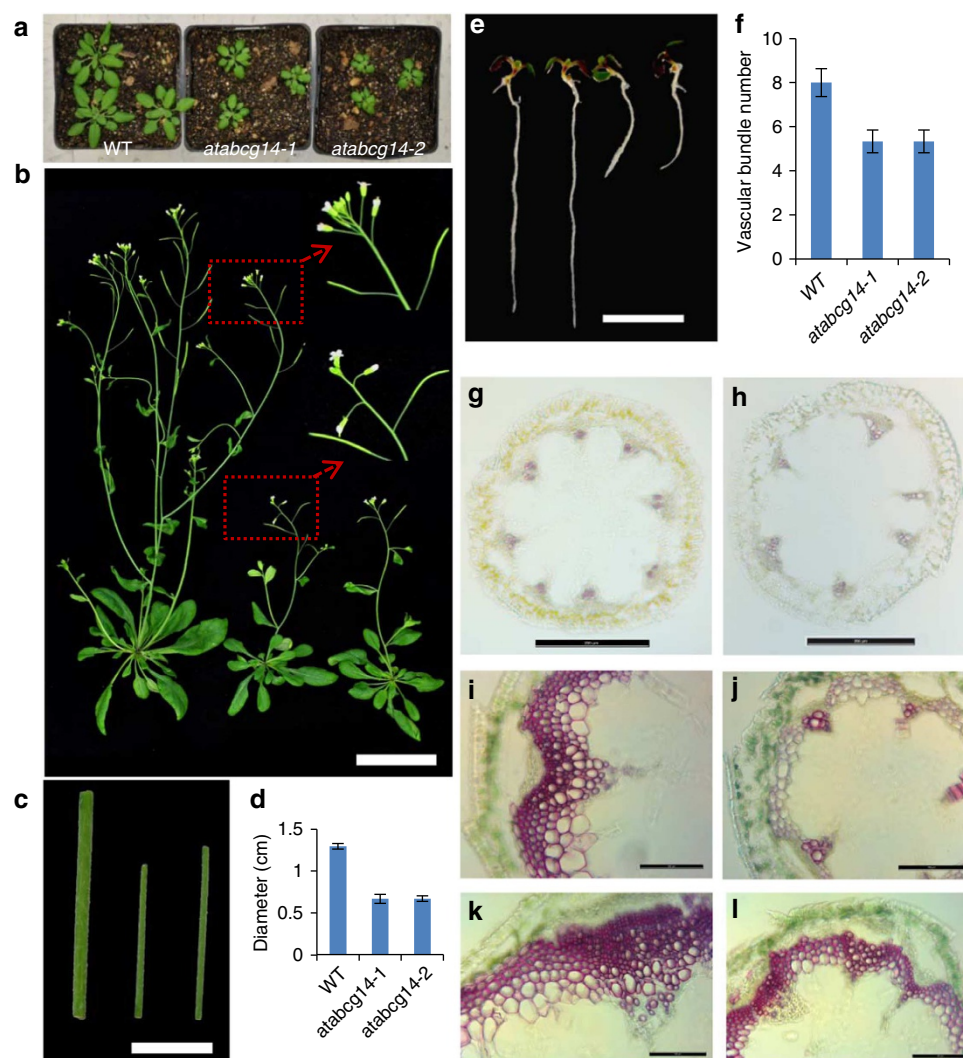
Figure 1 | Phenotypes of *atabcg14* mutants. (**a**) 25-DAG wild-type (left), *atabcg14-1* (middle) and *atabcg14-2* (right) mutant plants. (**b**) 35-DAG wild-type (left), *atabcg14-1* (middle) and *atabcg14-2* (right) mutant plants. Insets show wild-type inflorescences and the smaller *atabcg14-1* inflorescences (× 3 magnification). Scale bar, 5 cm. (**c**) Wild-type (left) and mutant (middle and right) stems. Scale bar, 1 cm. (**d**) Basal diameter of wild-type and *atabcg14* mutant stems (means ± s.d., n = 8). (**e**) Root elongation of 8-DAG wild-type (left two), *atabcg14-1* mutant (third from left) and *atabcg14-2* mutant (far right) seedlings. Scale bar, 1 cm. (**f**) Numbers of vascular bundles of wild-type and mutant plants (means ± s.d., n = 6). (**g**) and (**h**) Phloroglucinol staining of the top parts (below the third generated silique) of wild-type and *atabcg14-1* mutant inflorescences, respectively, illustrating the reduced numbers of vascular bundles in stems of the mutants. Scale bar, 200 μm. (**i**) and (**j**) Phloroglucinol staining of middle part (base of the third internode from the ground) of wild-type and *atabcg14-1* mutant stems, respectively. (**k**) and (**l**) Phloroglucinol staining of basal part (first internode from the ground) of wild-type and *atabcg14-1* mutant stems, respectively. Scale bars in (**i–l**), 100 μm.

numbers of cells in phloem and xylem in the vascular bundle were reduced; lignin synthesis and deposition (key processes in cell differentiation and secondary cell wall thickening) were considerably delayed, and the numbers of lignified cells were substantially reduced in the interfascicular fibres and xylem bundles of the mutant plants (Fig. 1i–l). This syndrome largely resembles secondary growth retardation observed in the *atipt1;3;5;7* quadruple mutant, where the key genes encoding ATP/ADP:isopentenyltransferases (*IPTs*) responsible for synthesizing cytokinins are disrupted, leading to low levels of cytokinins and reducing cambial activity in the shoot[4]. The altered secondary thickening of the *atabcg14* mutant points to a decline in fascicular- and interfascicular-cambial activity, implying a potential shortage of cytokinins in *atabcg14* shoots.

Besides the shorter primary roots and slender inflorescence stems, the mutant seedlings had shorter leaf petioles, smaller leaf areas and about 40% lower chlorophyll a and b contents than did wild-type plants, and thus were pale yellow rather than green (Supplementary Fig. 6). This is consistent with cytokinins' well-documented role in promoting chlorophyll retention[5,21], and further implies that *atabcg14* mutants have cytokinin deficiencies in their aerial tissues. Thus, the morphological, anatomical and physiological data collectively imply that disrupting *AtABCG14* interferes with the distribution and/or concentrations of cytokinins in both roots and shoots.

***atabcg14* impairs the acropetal distribution of cytokinins.** To verify whether AtABCG14 participates in controlling cytokinin distribution *in planta*, we monitored *GUS* expression, driven by *Arabidopsis* RR 5 promoter (*ARR5::GUS*), in the *atabcg14* mutant lines. *ARR5* is a type-A cytokinin RR gene of the two-component

system that is transcriptionally upregulated by cytokinins. Thus, changes in the concentrations of endogenous cytokinins affect its expression[22,27]. For demonstrating this, we crossed *atabcg14* with *ARR5::GUS* transformants and then examined GUS activity in seedlings of the homozygous cross-progenies (6 days after germination, 6-DAG). The progeny seedlings showed similar retardation in growth and losses in chlorophyll to the *atabcg14* mutant (Fig. 2a,b). The spatial expression patterns of *GUS* in the shoots and roots of *ARR5::GUS/atabcg14* seedlings sharply differed from those in *ARR5::GUS*/WT plants (Fig. 2c,d). In the wild-type background, *GUS* was abundantly expressed in the shoot/cotyledon leaves, and weakly expressed in the root cap's statocytes and the upward vascular cylinder. In contrast, GUS

activity was diminished by 71% in cotyledon leaves of *ARR5::GUS/atabcg14* seedlings, but strongly increased (about threefold) in their primary roots (Fig. 2e), where the GUS signals were widely distributed across all the cell types, including the cells of the epidermis, cortex and endoderm (Fig. 2d). These data clearly indicate that there are opposite patterns of cytokinin distribution in the roots and shoots of *atabcg14* and wild-type plants, and that cytokinin levels were low in shoots but high in roots of the mutants (Fig. 2e). Similarly, in the inflorescences of mature plants, GUS activity was substantially weaker in *ARR5::GUS/atabcg14* than in *ARR5::GUS*/WT plants (Fig. 2f). The GUS signals were clearly visible in the stigma, anther and receptacle of *ARR5::GUS*/WT plants, but undetectable in those of
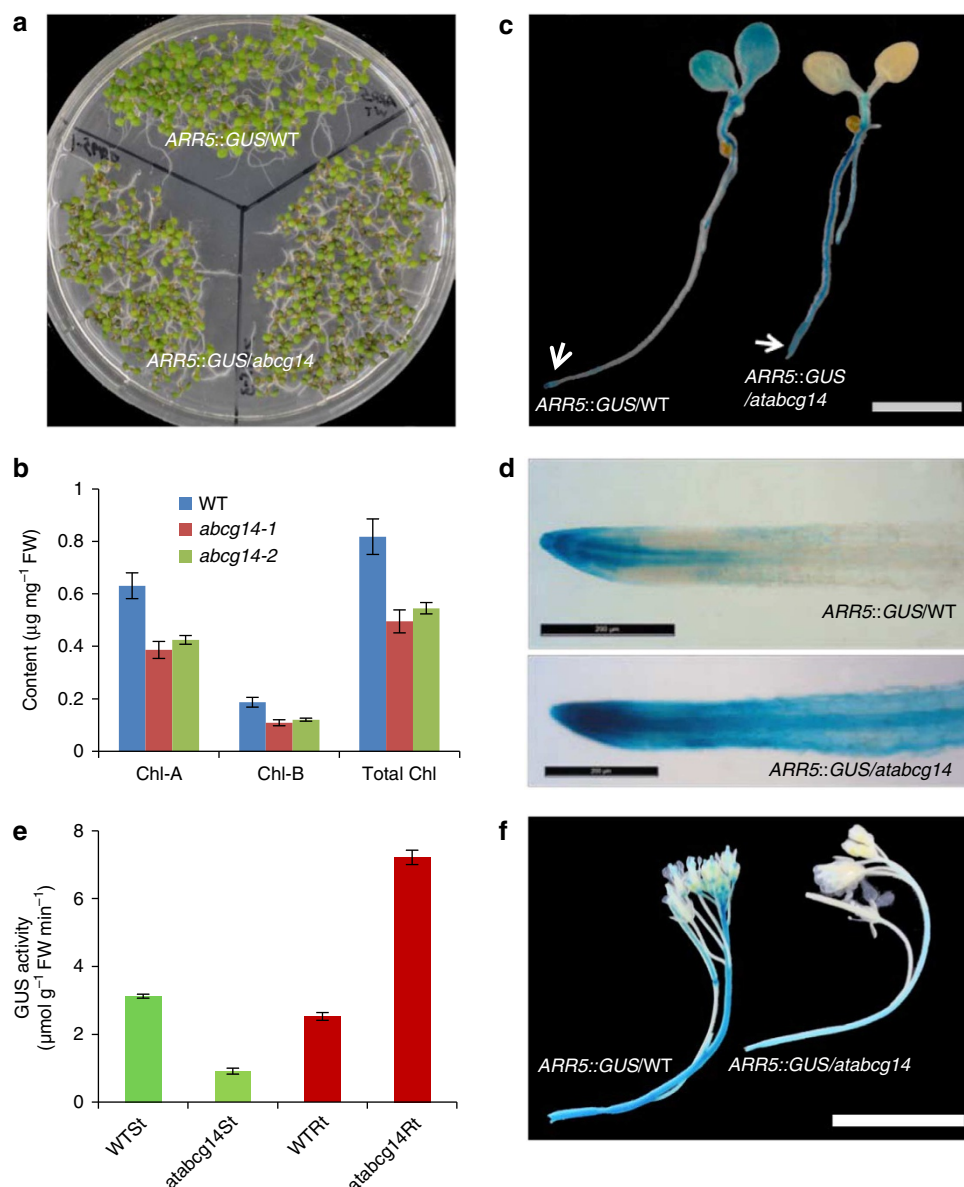
Figure 2 | Expression of *ARR5::GUS* reporter in *atabcg14* mutants. (**a**) Photograph illustrating phenotypes of 6-DAG *ARR5::GUS*/WT and *ARR5::GUS/atabcg14* seedlings. (**b**) Chlorophyll contents in 6-DAG *ARR5::GUS*/WT and *ARR5::GUS/atabcg14* seedlings. WT represents *ARR5::GUS*/WT; *atabcg1-1* and -2 represent *ARR5::GUS/atabcg14* lines 1 and 2, respectively. Chl-A, Chl-B and Total Chl represent chlorophyll a, chlorophyll b and total chlorophyll contents, respectively (means ± s.e., $n = 4$). (**c**) GUS staining (6 h) of *ARR5::GUS*/WT (left) and *ARR5::GUS/atabcg14* (right) seedlings. Note the distinct distribution of GUS signal in the shoot and root of wild-type and *atabcg14* plants. Arrows indicate the GUS staining in root tips. Scale bar, 0.5 cm. (**d**) Close-up of the portion of primary roots of *ARR5::GUS*/WT and *ARR5::GUS/atabcg14* plants arrowed in (**c**). Scale bars, 200 μm. (**e**) GUS activity (means ± s.e., $n = 3$) in shoots and roots of 8-DAG *ARR5::GUS*/WT and *ARR5::GUS/atabcg14* seedlings. St, shoot; Rt, root. (**f**) GUS staining (12 h) of *ARR5::GUS*/WT and *ARR5::GUS/atabcg14* inflorescences. Scale bar, 1 cm.

ARR5::GUS/atabcg14 plants (Supplementary Fig. 7). The altered spatial expression of *ARR5::GUS* in the *atabcg14* background strongly suggests that disruption of *AtABCG14* impairs the allocation of cytokinins between roots and shoots.

Altered distribution of *tZ*-type cytokinins in *atabcg14*. *tZ*-type cytokinins primarily are synthesized in the root and translocated to the shoot via the xylem flow[4]. Profiling the cytokinin species of *atabcg14* mutants by LC-MS/MS revealed fivefold reductions in the total levels of *tZ*-type cytokinins in their shoots, with corresponding increase in their roots, compared with wild-type controls (Table 1 and Supplementary Table 1). Particularly, *tZ* N_7-glucoside, the major storage form of *tZ*-type cytokinins in *Arabidopsis*, was reduced to < 20% of wild-type levels in *atabcg14* shoots, but were more than fourfold higher in the roots (Supplementary Table 1). In addition, the contents of DHZ-type cytokinins (metabolically derived from *tZ* precursors) were more than 62% lower than wild-type levels in shoots, with concomitant increases (up to tenfold) in the roots of the *atabcg14* mutants. These data demonstrate that knocking out AtABCG14 impairs the distribution of the root-synthesized *tZ*- and DHZ-type cytokinins in root and shoot. In contrast to the decline of both *tZ*- and DHZ-type cytokinins in the mutant shoots, the iP-type cytokinins (known to be synthesized in the shoots and transported via phloem flow) were increased in both the shoots and roots, as were the *cZ*-types that are synthesized from isopentenylated RNAs[28] (Table 1). This implicates an intrinsic homeostatic mechanism that plant cells may take to compensate for perturbations in synthesis and distribution of different types of cytokinins. Overall, these data indicate that AtABCG14 plays a key role in distribution of the root-synthesized *tZ*- or DHZ-type cytokinins *in planta*.

AtABCG14 expression in root pericycle and stelar cells. To further assess the function of *AtABCG14 in planta*, we investigated its expression pattern by using the 1.3-kb region 5′-upstream of the gene to drive expression of *GUS* or the enhanced green fluorescent protein (*EGFP*)-*AtABCG14* fusion cassette. Expression of the latter morphologically complemented the mutant phenotype (Supplementary Fig. 8), indicating that the selected upstream sequence represents a functional promoter and the EGFP-AtABCG14 fusion functions *in planta*. In 4-DAG seedlings, strong green fluorescent protein (GFP) signals appeared in the root and very weak signals in the shoot (Fig. 3a). In the primary root, GFP signals were primarily located in the pericycle and stelar cells (Fig. 3b,c). When examining *AtABCG14::GUS* expression in young seedling, the GUS staining was mainly detected in the transition and elongation/differentiation zones of the primary root, but was absent from its division zone (Fig. 3d). These findings are consistent with the reported spatial distribution and functional sites of cytokinins in roots[29]. Consistently, in the transition and elongation/

differentiation zones, GUS signals were also mainly detected in the pericycle and stelar cells (Fig. 3e). In plants approaching the bolting stage (25-DAG), *AtABCG14* was moderately expressed in the young rosette leaves in addition to the roots, especially in the midribs and veins (Fig. 3f,g). In the reproductive stage, *AtABCG14::GUS* expression was also detected in the open flowers, particularly in the mature anthers, and in siliques (Fig. 3h–j). Quantitative RT–PCR (qRT–PCR) analysis of 35-DAG plants in the reproductive stage showed that *AtABCG14* transcripts were mainly present in the root and inflorescence (Fig. 3k).

AtABCG14 localizes on the plasma membrane. So far, all the characterized ABCG proteins, except ABCG19, were localized to plasma membrane[30]. To probe the subcellular localization of AtABCG14, we transiently expressed the *35S::EGFP-AtABCG14* chimeric cassette in *Arabidopsis* leaf protoplasts. We noted that the fluorescence signals of the fusion protein primarily appeared in the rims of the protoplasts, just outside the clumps of chloroplasts that were located in the corner of cytoplasm (Fig. 4a). In sharp contrast, the free GFP expressed in the protoplasts appeared to be widely distributed inside the inner protoplast membrane, while the chloroplasts were dispersed within the fluorescent region (Fig. 4b). When the *35S::EGFP-AtABCG14* cassette was stably expressed in the *atabcg14* mutants, they were phenotypically rescued (Supplementary Fig. 9a). The fluorescence distribution of the fusion protein in leaf epidermal cells agreed well with that revealed by FM4-64 staining, a typical plasma membrane indicator[31], and also lined up with the adjacent cell wall that was labelled with propidium iodide (PI), the cell wall polysaccharide indicator[31] (Fig. 4c,d). Further, when we subjected the leaf cells to plasmolysis, the GFP signal co-segregated with FM4-64 staining (Supplementary Fig. 9b), whereas the GFP signal and PI staining separated when the leaf cells were similarly treated (Supplementary Fig. 9c). To further confirm AtABCG14's subcellular localization, we purified the plasma membrane fraction from *Arabidopsis* seedlings stably transformed with *35S::EGFP-AtABCG14* using an aqueous-polymer two-phase partitioning procedure[32]. Immunoblots with anti-GFP antibody revealed that the EGFP-AtABCG14 fusion dominated in plasma membrane preparation (upper phase), where the plasma membrane marker H^+-ATPase coexists (Fig. 4e and Supplementary Fig. 10). These microscopic observations and gel-blot analyses indicate that AtABCG14 is a plasma membrane-localized protein.

AtABCG14 transports the C^{14}-*tZ* tracer. To explore the involvement of AtABCG14 in translocating *tZ*-type cytokinins, we fed C^{14}-labelled *tZ* to the roots of wild-type and *atabcg14* mutant seedlings. We subsequently detected strong radioactivity in the shoots of wild-type plants, but only trace amounts in the mutants' shoots (Fig. 5a). However, radioactivity was enriched in their

Table 1 | Total cytokinin levels in shoots and roots of wild-type and *atabcg14* mutant plants.

Total CKs	WTSt	atabcg14-1St	atabcg14-2St	WTRt	atabcg14-1Rt	atabcg14-2Rt
tZ-types	67.05 ± 13.91	13.26 ± 1.48***	12.91 ± 0.51***	32.32 ± 2.61	130.21 ± 20.69***	155.37 ± 18.66***
cZ-types	10.04 ± 1.29	20.72 ± 4.63**	22.29 ± 1.61***	9.32 ± 1.27	6.46 ± 0.72**	6.42 ± 0.94*
DHZ-types	7.01 ± 1.31	4.36 ± 0.73*	4.79 ± 0.27*	6.24 ± 1.03	40.25 ± 2.16***	62.80 ± 10.83***
iP-types	33.32 ± 2.67	57.65 ± 2.14***	50.62 ± 0.76***	33.52 ± 4.25	51.84 ± 6.84**	59.56 ± 6.12***

CK, cytokinin; *cZ*, *cis*-zeatin; DHZ, dihydrozeatin; iP, isopentenyladenine; Rt, Root; St, Shoot; *tZ*, *trans*-zeatin.
Values in pmol g^{-1} fresh weight. Contents measured in ~20 mg freeze-dried samples of roots and shoots from 10-DAG *Arabidopsis* seedlings. Data are mean ± s.d., $n = 4$. Asterisks indicate statistically significant differences between mutant (*atabcg14-1* and *atabcg14-2*) and wild-type (WT) plants in one-way ANOVA analysis (*, ** and *** indicate *P*-values of 0.05 > *P* > 0.01, 0.01 > *P* > 0.001 and *P* < 0.001, respectively, from *t*-test).
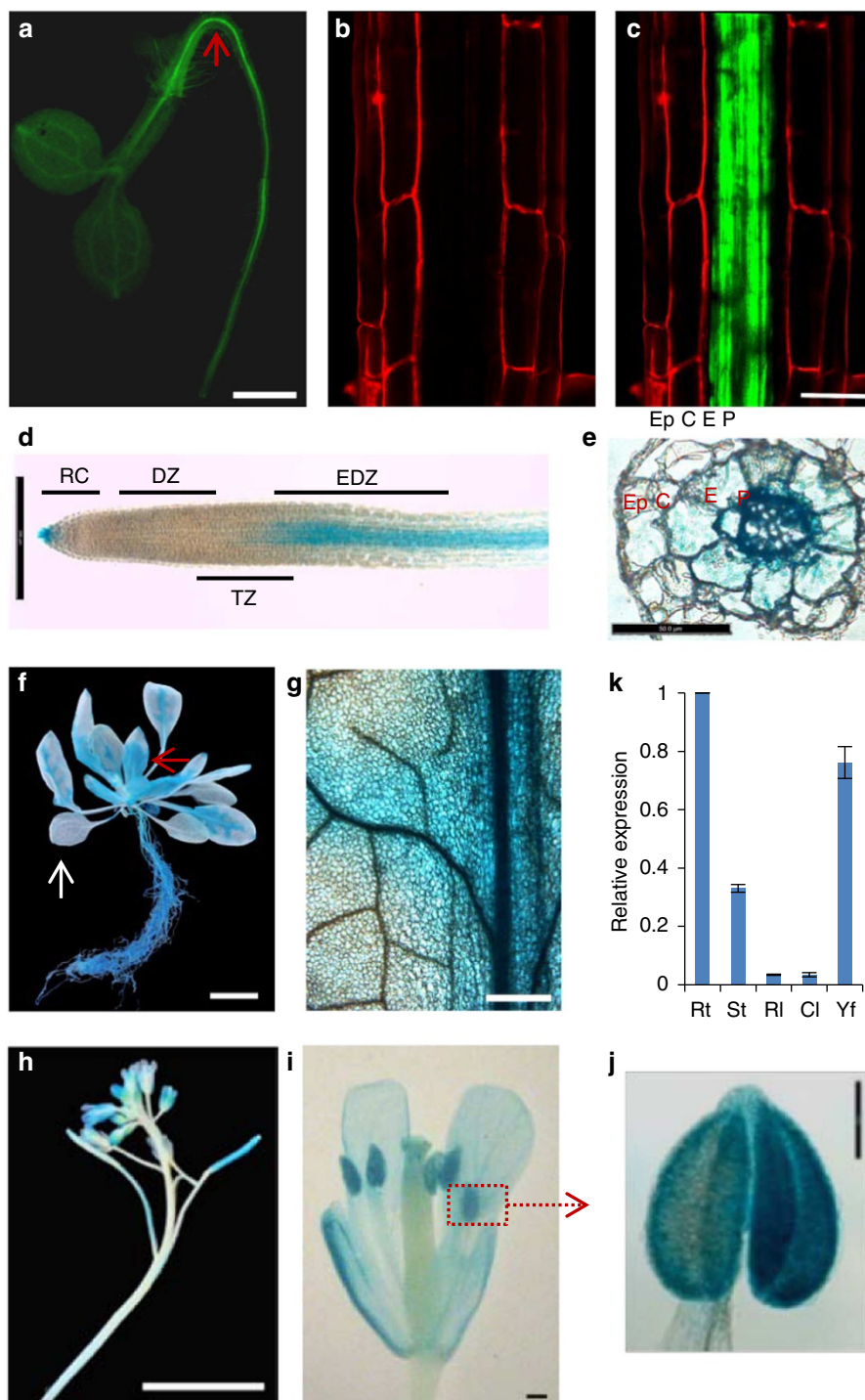
Figure 3 | Gene expression pattern and subcellular localization of AtABCG14. (**a**) Distribution of GFP signals in a 4-DAG *AtABCG14::EGFP-ABCG14* transgenic seedling. Arrow indicates the primary expression in roots. Scale bar, 500 μm. (**b**) and (**c**) PI staining of *AtABCG14::EGFP-ABCG14* transgenic roots (**b**) and merged image with GFP signal (**c**) observed under a confocal microscope, showing expression of *AtABCG14* in the pericycle and stelar cells in roots of (**a**). Scale bar, 25 μm. (**d**) GUS staining (6 h) in the root of a *AtABCG14::GUS* transgenic plant. RC, root cap; DZ, division zone; TZ, transition zone; and EDZ, elongation/differentiation zone. Scale bar, 200 μm. (**e**) Cross-section of the elongation zone of the primary root of an *AtABCG14::GUS* transgenic plant. Ep, epidermis; C, cortex; E, endodermis; P, pericycle. Scale bar, 50 μm. (**f**) GUS staining (12 h) of a 25-DAG *AtABCG14::GUS* transgenic plant. White and red arrows indicate an old leaf and a young, actively growing leaf, respectively. Scale bar, 1 cm. (**g**) The enlarged image of a GUS-staining leaf. Scale bar, 500 μm. (**h**) GUS staining (12 h) in the young inflorescence of an *AtABCG14::GUS* transgenic plant. Scale bar, 1 cm. (**i**) GUS staining (12 h) in the open flower of an *AtABCG14::GUS* transgenic plant. Scale bar, 100 μm. (**j**) GUS staining (12 h) in the mature anther from (**i**). Scale bar, 100 μm. (**k**) qRT–PCR analysis of *AtABCG14* expression in 35-DAG plants. Rt, root; St, stem; RL, rosette leaves; CL, cauline leaves; Yf, young inflorescence. The *ACTIN 2* gene was used as the control. Data are means ± s.e. (*n* = 3).
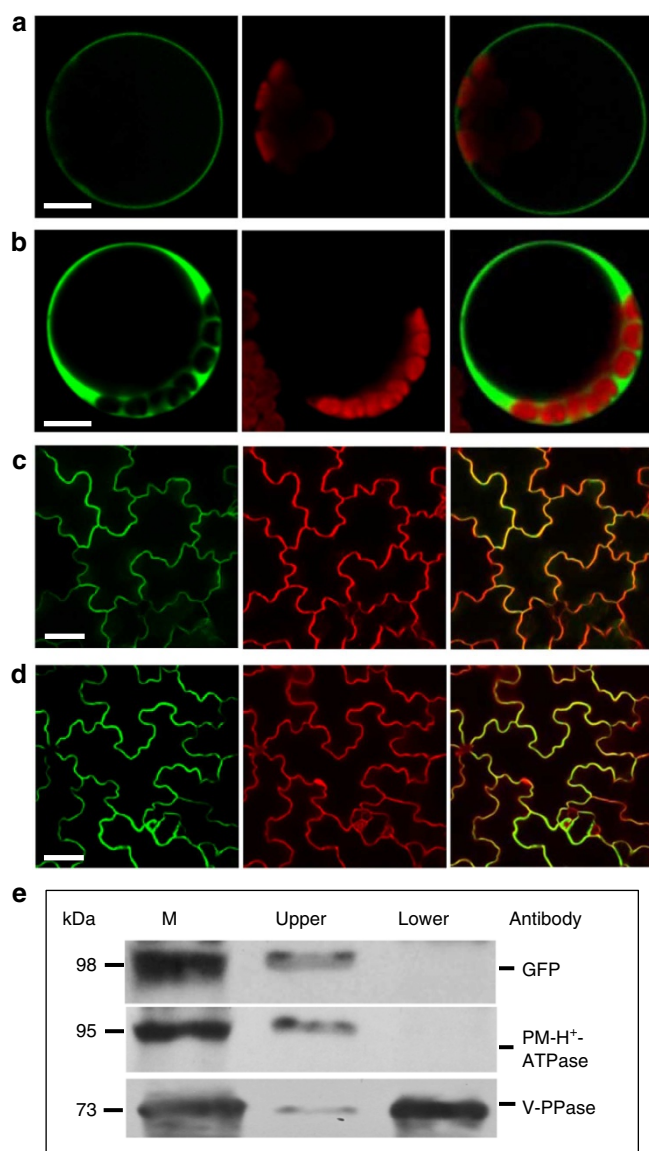
Figure 4 | Subcellular localization of EGFP-AtABCG14 fusion protein.
(**a**) and (**b**) Fluorescence distribution when *35S::EGFP-AtABCG14* (**a**) or
35S::EGFP (**b**) was expressed in tobacco leaf protoplasts (left);
autoflorescence of chloroplasts and merged images are shown in the
middle and right, respectively. Scale bar, 5 μm. (**c**) Distribution of
EGFP-AtABCG14 fluorescence in leaf epidermal cells (left), FM4-64
staining (middle) and merged image (right). Scale bar, 5 μm. (**d**)
Distribution of EGFP-AtABCG14 fluorescence in rosette leaf epidermal cells
(left), PI staining (middle) and merged image (right). Scale bar, 5 μm.
(**e**) Immunoblot analysis of membrane fractions from EGFP-AtABCG14
expressing seedlings by probing with antibodies against GFP, *Arabidopsis*
plasma membrane H$^+$-ATPase (PM-H$^+$-ATPase) and vacuolar
H$^+$-pyrophosphatase (V-PPase, tonoplast marker).

roots (Fig. 5b). In contrast, when S-adenosyl-L-C^{14}-methionine
was fed to the seedlings, as the control, it was effectively conveyed
from the roots to shoots in both wild-type and mutant plants, and
there was no clear difference in the distributions of radioactivity
(Fig. 5c,d). Furthermore, when C^{14}-*t*Z was fed to the functional
complementary lines (*atabcg14* mutants harbouring the *AtABC-
G14::EGFP-AtABCG14* cassette), the transport of C^{14}-*t*Z
to the shoots was not only completely restored but was about
2.5-fold higher than in wild-type plants (Fig. 5e). qRT–PCR

analysis revealed that the expression level of *AtABCG14* in this
complementary line was about sixfold higher than in the wild
type (Fig. 5f), presumably due to the presence of multiple copies
of the expression cassette. These data demonstrate a direct
correlation between C^{14}-*t*Z transport activity and the expression
level of *AtABCG14*. Furthermore, when both wild-type and
mutant seedlings were fed with C^{14}-*t*Z for a series of time periods,
the radioactivity progressively accumulated in the wild-type
shoots, whereas none or only negligible amounts of activity was
detected in those mutant lines over 5 h, a finding that further
suggests that a deficiency of AtABCG14 abolishes the transloca-
tion of C^{14}-*t*Z from root to shoot (Fig. 5g). To ascertain whether
the radioactivity detected in the fed seedlings represents *t*Z or its
derivatives, we fed the stable isotope tracer C^{13}-*t*Z to the roots of
both wild-type and mutant seedlings, and monitored its trans-
location and potential transformation by LC-MS. Over a 4-h
incubation period, the detected C^{13} labels in shoots pre-
dominantly either were the original form of C^{13}-*t*Z or its natural
derivatives such as the riboside, and *O/N*-glycoside, and they were
accumulated in wild-type shoots but nearly undetectable in the
mutant shoots (Table 2). Collectively, these data confirm the
involvement of AtABCG14 in *t*Z-type cytokinin transport from
root to shoot *in planta*.

ABC transporters can function either as importers or
exporters[16]. Thus, to further investigate the direction of
ABCG14-mediated transport of cytokinins, we incubated
detached leaves from 12-DAG transgenic seedlings harbouring
35S::EGFP-AtABCG14 (Supplementary Fig. 9a) with C^{14}-*t*Z,
followed by a thorough wash; we then detected the remaining
radioactivity in leaf cells. In plants harbouring *35S::EGFP-
AtABCG14*, AtABCG14 was expected to be expressed
ectopically in all types of cells, including the leaf epidermis as
shown by the GFP fluorescence distribution (Fig. 4c,d), whereas
the expression of ABCG14 in wild-type leaves was weak, and
restricted to the vein cells (Fig. 3a,f and g). Indeed, qRT–PCR
showed that the transcript level of *AtABCG14* is more than 250-
fold higher in the detached leaves of overexpression lines than in
wild-type control (Fig. 6a). Accordingly, the accumulated
C^{14}-radioactivity in leaf cells of the transgenic plants was four
times lower than in wild-type controls (Fig. 6b). In contrast, the
uptake of C^{14}-SAM did not markedly differ between transgenic
and wild-type leaves (Fig. 6c). Moreover, pre-treatment of the
detached leaves with the specific inhibitor of the ABC type
transporter, sodium *ortho*-vanadate, substantially mitigated the
loss of radioactivity in the cells harbouring *35S::EGFP-AtABCG14*
(Fig. 6b). Furthermore, throughout the incubation period
with C^{14}-*t*Z, the difference in the accumulated radioactivity
between wild-type and transgenic leaf cells remained constant
(Fig. 6d).These data corroborate that the less uptake of the
transgenic leaf cells to the fed radiotracer is attributed to
AtABCG14 activity and that AtABCG14 likely functions as an
exporter for the fed tracer.

Discussion

Cytokinins can act as autocrine, paracrine or long-distance
signals[1,10], and different types of cytokinins are synthesized and
distributed in distinct tissues or cell types. Several cytokinin
biosynthetic genes are found mainly expressed in the root, for
instance, *AtIPT1* and *AtIPT7* are primarily expressed in the
vascular stele of the elongation zone and/or root phloem
companion cells, indicating that these sites are major sources of
root-derived cytokinins[33]. Moreover, the xylem sap of several
plant species predominantly contains *t*Z-type cytokinins,
especially *t*Z riboside (*t*ZR)[10,34]. These data suggest that
the roots, particularly the root pericycle and phloem company
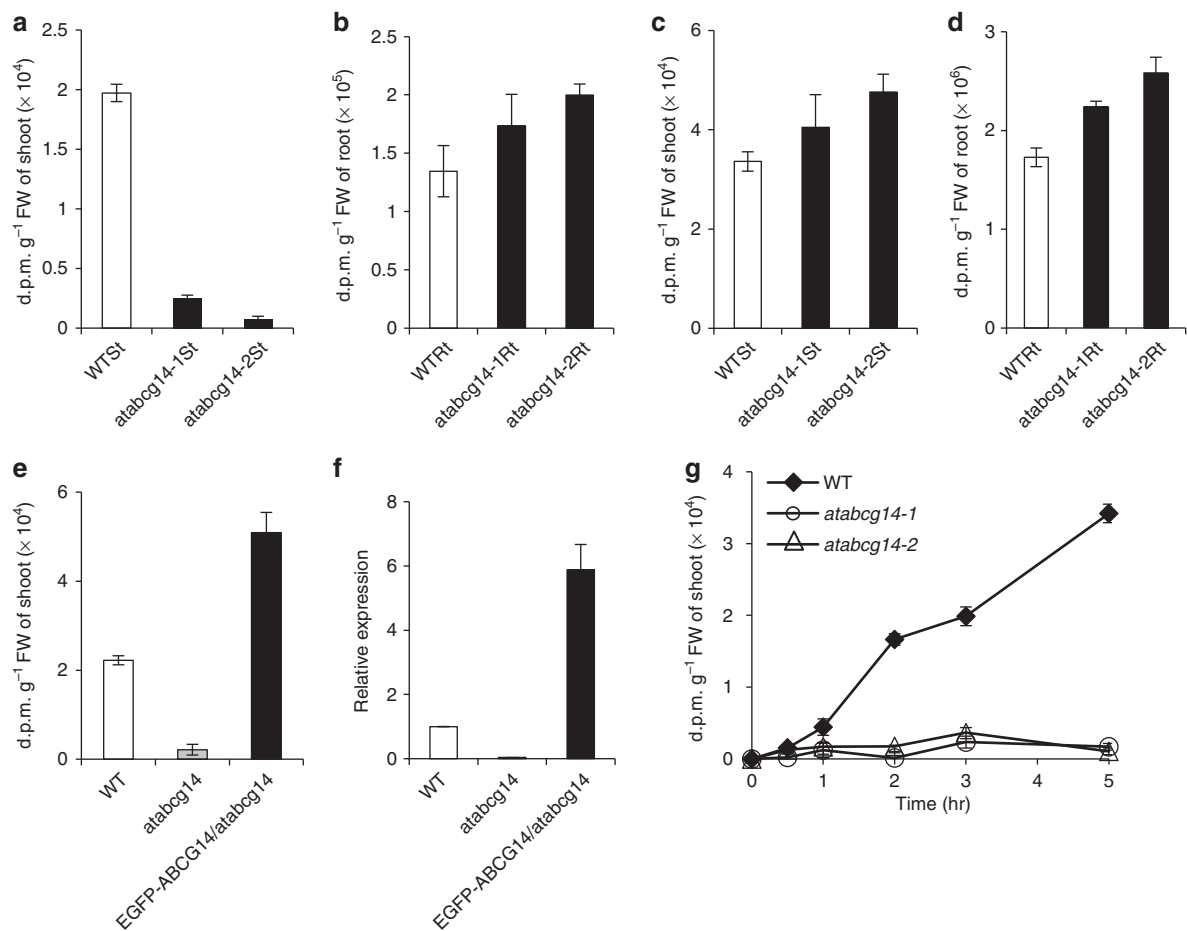
Figure 5 | Effect of AtABCG14 on translocation of cytokinin from root to shoot. Radioactivity in the following organs of wild-type and *atabcg14* mutant seedlings: (**a**) shoots (St) after feeding C^{14}-*t*Z to their roots (Rt); (**b**) roots after feeding C^{14}-*t*Z to their roots; (**c**) shoots after feeding S-adenosyl-*L*-C^{14}-methionine (C^{14}-SAM) to their roots; (**d**) roots after feeding C^{14}-SAM to their roots. (**e**) Radioactivity in shoots of wild-type, *atabcg14* and seedlings harbouring *AtABCG14::EGFP-AtABCG14* cassette after feeding C^{14}-*t*Z to their roots; (**f**) the relative expression levels of the *AtABCG14* in wild-type, *atabcg14* and seedlings harbouring *AtABCG14::EGFP-AtABCG14* cassette. The *UBIQUITIN 10* gene was used as the control. Data are means ± s.d. ($n = 3$); (**g**) radioactivity in shoots of wild-type and *atabcg14* mutant seedlings after feeding C^{14}-*t*Z to their roots in a time course. Data in (**a**–**e**) and in (**g**) are means ± s.e. ($n = 3$).

Table 2 | The detected C^{13}-labelled species in shoots and roots of wild-type and *atabcg14* mutant fed with C^{13}-*t*Z.

Total CKs	WTSt	atabcg14St	WTRt	atabcg14Rt
[$^{13}C_5$]*t*Z	1.1 ± 0.5	0.02 ± 0.0*	44.2 ± 11.1	88.8 ± 25.3*
[$^{13}C_5$]*t*ZR	6.2 ± 2.2	0.01 ± 0.0*	4.9 ± 0.3***	22.5 ± 2.3***
[$^{13}C_5$]*t*ZR5′MP	n.d.	n.d.	2.1 ± 0.5	10.8 ± 2.7*
[$^{13}C_5$]*t*ZOG	n.d.	n.d.	4.0 ± 1.2	4.1 ± 0.9**
[$^{13}C_5$]*t*ZROG	n.d.	n.d.	0.1 ± 0	0.2 ± 0.0
[$^{13}C_5$]*t*Z7G	1.0 ± 0.1	0.7 ± 0.2	66.6 ± 15	109.1 ± 14.7*
[$^{13}C_5$]*t*Z9G	0.2 ± 0	n.d.	6.4 ± 1.2	12.4 ± 1.6***

CK, cytokinin; n.d., not detected; Rt, Root; St, Shoot; *t*Z, *trans*-zeatin; *t*ZOG, *trans*-zeatin *O*-glucoside; *t*ZR, *trans*-zeatin riboside; *t*ZR5′ MP, *trans*-zeatin riboside 5′ monophosphate; *t*ZROG, *trans*-zeatin riboside *O*-glucoside; *t*Z7G, *trans*-zeatin 7-glucoside; *t*Z9G, *trans*-zeatin 9-glucoside.
Values in pmol g^{-1} fresh weight. Contents (means ± s.d., $n = 4$) measured in ∼20 mg freeze-dried samples of roots and shoots from 10-DAG *Arabidopsis* seedlings fed with 5 nM [$^{13}C_5$]*t*Z for 4 h.
Asterisks indicate statistically significant difference in the mutant line versus the wild-type (WT) in one-way ANOVA analysis (*, ** and *** correspond to *P*-values of $0.05 > P > 0.01$, $0.01 > P > 0.001$ and $P < 0.001$, respectively, from *t*-test).

cells, are the main sites of *t*Z production and that *t*ZR might act as an acropetal signal. In contrast, iP- and *c*Z-types are the main cytokinins in phloem sap, where they might function as basipetal or systemic signals[10,33,34].

Members of the purine permease family[11,12] and ENT family[10,14] hypothetically are involved in cytokinin transport.

One of the former, AtPUP1, is reportedly expressed in the epithelium of hydathodes, and the stigma surface, suggesting a potential role in retrieving cytokinins from xylem sap, thus preventing losses during guttation, while AtPUP2 is expressed mainly in phloem, implying a role in long-distance transport of phloem cytokinins[11,12]. The ENT transporters putatively mediate
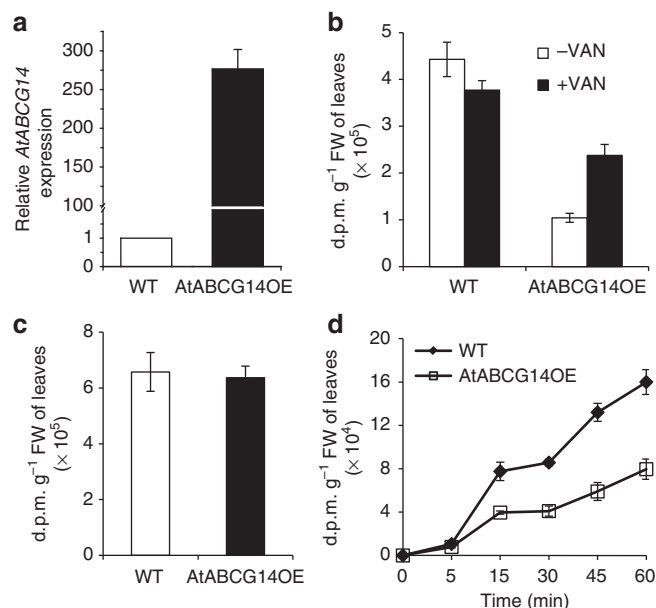
Figure 6 | AtABCG14 cytokinin (*trans*-zeatin) transport activity. (**a**) The relative expression levels of the *AtABCG14* in the leaves of wild type and an overexpression line harbouring *35S::EGFP-AtABCG14* (AtABCG14OE). The *UBIQUITIN 10* gene was used as the control. Data are means ± s.d. (*n* = 3). (**b**) Radioactivity in the detached leaves of wild-type plants and overexpression line after feeding with C^{14}-*tZ* in the presence or absence of 1 mM sodium vanadata for 1 h. (**c**) Radioactivity in the detached leaves of wild-type plants and overexpression line after feeding with C^{14}-SAM. (**d**) Radioactivity in the detached leaves of wild-type plants and over-expression line after feeding with C^{14}-*tZ* over a time course. Data in (**b**–**d**) are means ± s.e. (*n* = 3).

translocation of adenosine and other nucleosides, including iPR and *tZR*[10,14]. Both of these types of transporters were implicated to be involved (based on *in vitro* data), as cytokinin importers, in the maintenance of either nucleobase homeostasis, or the phloem flow of cytokinins. However, definitive *in planta* proof is lacking of their role in cytokinin transport. Several lines of evidence obtained in the present study strongly indicate that AtABCG14, a previously uncharacterized half-molecule ABC family member, plays a pivotal role in the long-distance translocation of root-synthesized *tZ*- and DHZ-type cytokinins in *Arabidopsis*. This evidence includes the following: the morphological and physiological perturbations exhibited in the *atabcg14* mutant alleles, the predominant pericycle gene expression pattern of *AtABCG14*, the plasma membrane localization of the encoded protein, the disturbed distribution of cytokinins in roots and shoots of the *atabcg14* null mutants and the close correlation of the translocation of exogenously supplied C^{14}-*tZ* with the activity of AtABCG14. In particular, knocking out *AtABCG14* almost completely diminished the translocation of the fed radio-tracers from the root to shoot over the entire incubation period, while the complementation of gene expression completely restored their transport (Fig. 5). Moreover, the root-to-shoot transport activity to C^{14}-*tZ* is closely proportionate to the levels of *AtABC14* expression in the wild-type, mutant and complementary (or overexpression) lines (Figs 5 and 6). Finally and more definitively, the transport assays using detached leaves showed that transgenic cells with high-level constitutive expression of AtABCG14 exhibited significant efflux activity to the fed C^{14}-*tZ*, and that such activity was sensitive to the application of sodium vanadate, the specific ABC transporter inhibitor (Fig. 6); together, these findings substantiate the involvement of AtABCG14 in

transporting *tZ*-type cytokinins. Therefore, ABC transporters represent a novel family of transporters for cytokinin compartmentalization *in planta*. The exact transporting form of *tZ*-type cytokinins mediated by the action of AtABCG14 remains undetermined. Our attempt to determine AtABCG14's biochemical properties *in vitro* was unsuccessful. This is probably due to the assay systems that we adopted were not optimal for the effective functional detection or due to the transporter's half-molecular nature and the possible requirement for an unknown hetero-partner for its proper functioning[31]. These technical obstacles currently prevented our unequivocal assessment of its biochemical function; nevertheless, our transport activity assay using detached leaves, in which one set of leaf cells, as the control, was from a wild-type background that showed very low level of (or even negligible) expression of AtABCG14, and the other set of leaves harboured the overexpressed AtABCG14 (about 250-fold higher in its transcripts, compared with the control leaves), does closely resemble a conventional *in vitro* assay system for examining this transporter's function. In addition, monitoring the fed stable isotope in seedlings by LC-MS clearly links the translocation of the fed *tZ* (and its derivatives) with the necessity of existence of AtABCG14 in cells (Table 2). Therefore, our comprehensive C^{14} and C^{13} tracer feeding experiments *in planta* and our 'semi'-*in vitro* transport assay using detached leaves provided essential genetic and biochemical evidence showing that AtABCG14, as an exporter, likely functions in transporting/distributing *tZ*-type cytokinin species.

The promoter of *AtABCG14* drove GFP or GUS expression in the root's pericycle and stelar cells (Fig. 3b,c,e). This finding is reminiscent of the expression pattern of the *BOR1* exporter that is predominantly expressed in the root's pericycle cells and is responsible for xylem loading of boric acid[35]. Therefore, the presence of AtABCG14, as an efflux pump therein, most likely is involved in transferring root-synthesized cytokinins into the xylem for their long-distance translocation. Besides the predominant expression in the pericycle and stelar cells of the root-elongation zone, like many other genes involved in cytokinin biosynthesis, *AtABCG14* was also expressed in inflorescence/open flowers, siliques and the young leaves. Its precise physiological functions in these tissues are still unknown. However, as an efflux pump, the presence of AtABCG14 in diverse tissues implies that it may also participate in the paracrine (transcellular) transport of cytokinins to the apoplast or neighbouring cells, in addition to xylem loading in the roots.

Interestingly, root elongation in *atabcg14* mutants is less sensitive to exogenous cytokinins than that it is in wild-type plants (Supplementary Fig. 5). Although this characteristic phenotypically resembles the behaviour of cytokinin receptor mutant line *cre1/ahk4*, in which the perception of cytokinin signals is defective in the root[36], mechanistically it may be quite distinct. One possible explanation is that the already high abundance of cytokinins in roots of *atabcg14* mutants, resulting from the defect in root-to-shoot translocation (Table 1), may compromise the sensitivity of the root meristem cells in perceiving the exogenously applied signal molecules. Further study is needed to clarify this.

We believe that the presented findings have important practical implications. Cytokinins delay leaf senescence, thereby extending the photosynthetic period[5,6,21] and enhancing the plant's photosynthate production capacities. They also play key roles in regulating reproductive development and sink strength[37,38]; thus, they are among the most important target hormones for improving crop yields. Furthermore, they are pivotal signals in communicating nitrogen availability from roots to shoots via the xylem vessels[10,33]. However, the regulation of their distribution in

plants is poorly understood. We identified and characterized AtABCG14 as a key player in the long-distance transport of cytokinins, particularly *t*Z (the commonest cytokinin in higher plants, and highly active in receptor assays and bioassays[39]). This finding will provide insight into the molecular mechanisms involved in cytokinin partitioning. Moreover, the results may open new avenues for modifying various important crops, agriculturally, biotechnologically and horticulturally, to increase yields and reduce fertilizer requirements for instance, while improving the exploitation of sustainable bioenergy resources.

Methods

Plant materials and growth conditions. *Arabidopsis thaliana* ecotype Columbia was used as the wild type for all experiments. The T-DNA insertion lines SK_15917 and SK_15918 were obtained from the *Arabidopsis* Biological Resource Center. *ARR5::GUS* and *CYCB1;1::uidA* transgenic seeds were kindly provided by Drs Thomas Schmülling (Free University of Berlin) and Peter Doerner (University of Edinburgh), respectively. Seeds were sown on petri dishes containing half-strength MS with 0.25% phytogel or 0.7% w/v phytoagar and appropriate antibiotics, then kept at 4 °C for 3 days before being moved to a growth chamber. Seedlings with two true leaves were transplanted into soils. Wild-type, mutant and/or transgenic plants were grown side by side in the same tray to minimize possible variations in growth conditions. Plants were grown at 22 °C in a growth chamber under a long-day regime (16-h light/8-h dark) unless otherwise stated. The seedling root elongation assay was performed in a growth chamber at 22 °C under a 14-h light/10-h dark regime.

Identification of T-DNA insertion atabcg14 null mutants. The T-DNA specific primer pSKTAIL-L1 and the gene-specific primers ABCG14-P1 and ABCG14-P2 were used to identify homozygous *atabcg14* mutants at genomic DNA and transcriptional levels, respectively. All primers used in this study are listed in Supplementary Table 2.

Phenotyping and histochemical analysis. The diameter of the basal primary stem was measured using a Vernier caliper. Histochemical analysis was performed using 30-μm-thick sections from stems at the same position of wild-type and *atabcg14* mutants following the standard protocols of phloroglucinol staining[40]. The number of vascular bundle was calculated based on the observation from the young (top) stems.

Vector construction. The coding region of the *AtABCG14* gene amplified by primers ABCG14-P3 and ABCG14-P4 was cloned into gateway entry vector pDONR207 to form pDONR207-ABCG14 via BP reaction. To construct 35S::ABCG14 and 35S::GFP-ABCG14 binary vectors, the *AtABCG14* in pDONR207-AtABCG14 was introduced into pMDC32 and pMDC43, respectively, via LR reactions.

To make 35S::EGFP-ABCG14 and AtABCG14::EGFP-ABCG14 constructs, the *ABCG14* coding region was amplified by primers ABCG14-P5 and ABCG14-P6 then cloned into the EGFP vector of pSAT6-GFP-N1 (ref. 41) at the EcoRI and BamHI restriction sites to form pSAT6-35S::EGFP-ABCG14. The 35S promoter of pSAT6-35S::EGFP-AtABCG14 was then replaced by the *AtABCG14* promoter amplified by ABCG14-P7 and ABCG14-P8 from genomic DNA at AgeI and NcoI sites to form the shuttle vector pSAT6-AtABCG14::EGFP-ABCG14. 35S::EGFP-ABCG14 and ABCG14::E GFP-AtABCG14 expression cassettes were released from the pSAT6 shuttle vectors with PI-PspI, and subcloned into the binary vector pPZP-RCS2 to form binary vectors pPZP-35S::EGFP-ABCG14 and pPZP -ABCG14::EGFP-ABCG14, respectively.

To make the genomic complementary construct G-ABCG14, a 4.1 kb genomic fragment was amplified by primers ABCG14-P9 and ABCG14-P10. The amplified fragment was digested by EcoRI and ligated to the EcoRI sites of pZP211 to form the G-ABCG14 construct.

The *AtABCG14* promoter was amplified by primers ABCG14-P11 and ABCG14-P12. The promoter region was then cloned into the pDONR207 entry vector via the BP reaction, designated pDONR207-pABCG14. To make the ABCG14::GUS and ABCG14::EGFP constructs, the promoter region of *ABCG14* in pDONR207-pABCG14 was ligated into pMDC163 and pMDC107, respectively, via LR reactions. All the constructs described above were confirmed by sequencing.

Hormone treatments. Hormone treatments followed the method of Inoue *et al.*[36] with minor modifications. Briefly, seeds of selected genotypes were sown on half-strength MS medium containing BA, *t*Z, ACC or NAA with various concentrations. After chilling for 3 days, the plates were vertically incubated at 23 °C for 8 days and their root lengths in digital images were measured by Image J software (1.43). We calculated the relative root lengths by comparison with those of corresponding seedlings grown in hormone-free medium. The data presented are the mean of measurements from at least 12 plants.

Determination of subcellular localization of ABCG14. Protoplasts isolated from young leaves of *Arabidopsis* plants grown under a 14 h light/10 h dark regime were transformed with column-purified plasmid DNA as previously described[42]. After 24-h incubation in the dark, the protoplasts were analysed for the presence of green fluorescence.

10-DAG transgenic seedlings harbouring 35S::EGFP-ABCG14 were used for protein localization. Cotyledon leaves and the first pair of true leaves were stained with 1 μg ml^{-1} PI (Sigma-Aldrich) or 10 μM FM4-64 (Molecular Probes) for 10 ~ 30 min. Cells in the leaves were also plasmolysed in 30% sucrose solution for about 1 h before staining in PI or FM4-64 in a 30% sucrose solution. Images were captured using a Leica DMI6000 microscope. GFP was detected using a 488-nm laser with a 505–530 nm filter. PI and FM4-64 staining were detected using a 488-nm laser with a 600–650 nm filter. Images were processed by Adobe Photoshop 8.0 (Adobe Systems, Mountain View, CA).

Membrane preparation and gel-blot analysis. Microsome preparation was followed the procedure described in Miao and Liu[43]. Briefly, *Arabidopsis* seedlings (12-DAG) harbouring 35S::EGFP-AtABCG14 expression cassette were ground with 50 mM Tris buffer A (pH 8.0) containing 2 mM EDTA, 20% Glycerol, 1 mM DTT and a 1X Protease inhibitor cocktail (PIC). The homogenate was filtered through Miracloth and centrifuged twice at 5,000 g for 15 min to remove the debris. Supernatants were centrifuged at 100,000 g for 1 h to pellet the microsomal membranes. The resulting microsomes were resuspended in 5 mM potassium phosphate buffer B (pH 7.8) containing 330 mM sucrose, 5 mM KCl, 1 mM DTT and 0.1 mM EDTA and 1X PIC. The plasma membranes were purified further from the microsomal preparation by partitioning in an aqueous-polymer two-phase system according to Larsson *et al.*[32] Briefly, the final weight of 9 g microsomal preparation in buffer B was added to 27 g of buffer C containing 5 mM potassium phosphate (pH 7.8), 330 mM sucrose, 5 mM KCL, 1 mM DTT, 0.1 mM EDTA, 1X PIC, 8.6% (w/w) Dextran T500 and 8.6% (w/w) polyethylene glycol 3,350, then mixed and partitioned by about 50 inversions. The two phases were separated by spinning at 1,500 g for 4 min. The resulting upper and lower phases were diluted using buffer B (pH 7.8) for three times and ten times, respectively, and centrifuged at 100,000g for 2 h to obtain the membrane pellets. All procedures above were performed at 4 °C. The two-phase pellets as well as total microsomes were resuspended in 1X SDS buffer, heated at 70 °C for 10 min and developed on 10% SDS–PAGE gel. Immunoblots were probed with antibodies against GFP (Invitrogen A6455), *Arabidopsis* plasma membrane H$^+$-ATPase (Agrisera AS07-260), vacuolar H$^+$-pyrophosphatase (Operon Biotechnologies COP-080001), according to the standard procedure of gel blot. The cropped and full immunobloting images are presented in Fig. 4 and Supplementary Fig. 10, respectively.

Gene expression analysis. Total RNA was prepared from *Arabidopsis* flower tissues using Trizol reagent (Invitrogen). To remove any contaminating DNA, the samples were treated with DNase (RNase-free DNase Kit; Promega). The reverse transcriptional reaction was performed using M-MLV Reverse Transcriptase (Promega). Quantitative PCR was undertaken using a MyIQ-Cycler (Bio-Rad) and IQ SYBR Green Supermix (New England Biolab) according to the manufacturer's instructions with the following cycles: 10 min at 95 °C, followed by 40 cycles of 15 s at 95 °C, 25 s at 58 °C and a final extension of 40 s at 72 °C. The gene-specific primers ABCG14-P1 and ABCG14-P2 were used in RT–PCR to amplify the *AtABCG14* gene, in which the *ACTIN 2* gene was amplified by primers Actin 2F and Actin 2R as the control. For qRT–PCR, the *AtABCG14* gene-specific primers ABCG14-P13 and ABCG14-P14 were used, the *ACTIN 2* gene amplified with Actin 2QF and Actin 2QR or *UBIQUITIN 10* gene amplified with Ub10F and Ub10R primers was used for quantitative normalization. The expression level of *AtABCG14*, after normalization to that of *ACTIN 2* or *UBIQUITIN 10* control gene, is expressed as the relative value to the highest level in root tissue (in Fig. 3k) or to the level in wild-type seedlings (Figs 5f and 6a) that was expressed as a value of 1.

GUS staining and light microscopy. Histochemical analysis of the GUS reporter enzyme was performed according to Jefferson *et al.*[44] with minor modifications. Briefly, tissues from transgenic plants were collected in glass vials containing ice-cold 90% acetone and incubated for 30 min at room temperature, then transferred into the reaction buffer and incubated for 1 to 12 h at 37 °C. After staining, pigments in the samples were destained with 70% ethanol, and the GUS staining pattern was recorded with a digital camera (Nikon DC3000) or a microscope (Leica DM5500B). For sectioning, plant tissues were fixed with formalin-acetic acid-alcohol (1.8% formalin, 5% acetic acid and 90% methanol) and embedded in paraffin; 8-μm thick sections were cut.

Cytokinin profiling. *Arabidopsis* seeds of selected genotypes were grown on half-strength MS medium supplemented with 3% sucrose. 10-DAG seedlings were used for cytokinin profiling. The roots and shoots of the seedlings were separated carefully with a razor at the junction between roots and hypocotyls. Approximately 20 mg fresh roots or shoots were freeze-dried in a microtube with a screw cap. The cytokinin extraction and profiling essentially followed a previously described method[28]. Briefly, the plant materials in 2.0 ml micro-centrifuge were mixed with

the following stable isotope-labelled cytokinin internal standards at a concentration of 0.5 pmol of each compound per 50 µl of Bieleski buffer: $[^{13}C_5]cZ$, $[^{13}C_5]tZ$, $[^2H_5]tZR$, $[^2H_5]tZ7G$, $[^2H_5]tZ9G$, $[^2H_5]tZOG$, $[^2H_5]tZROG$, $[^2H_5]tZMP$, $[^2H_3]DHZ$, $[^2H_3]DHZR$, $[^2H_3]DHZ9G$, $[^2H_7]DHZOG$, $[^2H_3]DHZMP$, $[^2H_6]iP$, $[^2H_6]iPR$, $[^2H_6]iP7G$, $[^2H_6]iP9G$ and $[^2H_6]iPMP$. They then were extracted in Bieleski solvent using a MM 301 vibration mill (Retsch GmbH & Co. KG, Haan, Germany). The tube's contents were ultrasonicated and then incubated for 30 min at 4 °C. After centrifugation, the supernatants were transferred onto StageTips and purified according to the protocol described in Svacinova et al.[28] After elution, we collected the eluates and evaporated them to dryness in a Speed-Vac concentrator RC1010 (Jouan, Winchester, UK). Thereafter, we dissolved them in 20 µl of 10% methanol, and 10 µl of each sample was injected on to a reversed-phase column (Acquity UPLCW BEH C18, 1.7 µm, 2.1 mm × 150 mm, Waters). The samples were eluted in a 24-min gradient composed of methanol (A) and 15 mM ammonium formate pH 4.0 (B) at a flow rate of 0.25 ml min^{-1}, with a binary gradient: 0 min, 5:95 (A:B); 7.0-min isocratic elution, 5:95 (A:B); 9.0-min linear gradient, 20:80 (A:B); 7.0-min linear gradient, 50:50 (A:B) and 1 min isocratic elution, 50:50 (A:B). The effluent was passed through an ultraviolet-diode array detector and the tandem mass spectrometer Xevo TQ MS without post-column splitting. The parameter settings were followed as described previously[28]. We quantified them using a standard isotope-dilution method. We determined the ratio of endogenous cytokinin to the appropriate labelled standard and further quantified the level of endogenous compounds in the original extract, according to a known quantity of an added internal standard.

Cytokinin tracer-uptake assay. *Arabidopsis* seeds of selected genotypes were grown on half-strength MS medium supplemented with 3% sucrose. 10∼12-DAG seedlings were used for the in planta isotope feeding. For root-feeding experiments, the root tips of *atabcg14* mutants, the complementary line harbouring *AtABC-G14::EGFP-AtABCG14* and wild-type seedlings were immersed in 5 mM MES-KOH (pH 5.6) buffer containing C^{14}-*tZ* (American Radiolabeled Chemicals, 3,700 Bq ml^{-1}, final concentration 5 nM) or S-adenosyl-L-C^{14}-methionine (American Radiolabeled Chemicals, 3,700 Bq ml^{-1}, final concentration 5 nM) as a control. After 4 h, the roots and shoots of the seedlings were carefully separated using a razor at the junction between roots and hypocotyls. The shoots and roots from three seedlings of each genotype were pooled (separately) as replicates. The roots were washed again with 1 ml 5 mM MES-KOH (pH 5.6) buffer three times. For the time–course feeding experiment, the root tips of both wild-type and mutant seedlings were incubated with 5 nM C^{14}-*tZ* in 5 mM MES-KOH (pH 5.6) buffer for 0.5, 1, 2, 3 and 5 h, and the shoots of seedlings were collected. The seedling samples were then mixed with 200 µl bleach and incubated at 55 °C for 2 h to solubilize the tissues. Radioactivity was quantified by a scintillation counter.

For stable C^{13}-*tZ* feeding, 12-DAG wild-type and mutant seedlings were incubated with 5 nM stable labelled chemical in 5 mM MES-KOH (pH 5.6) buffer for 4 h. The roots and shoots from 4∼6 seedlings were separated, weighed and freeze-dried in a microtube with a screw cap for processing their extraction and analysis by LC-MS[28].

To feed C^{14}-*tZ* or -SAM into the detached leaves, cotyledon leaves and the first pair of true leaves from three to five 10∼12-DAG seedlings of the wild type and overexpression line harbouring *35S::GFP-AtABCG14* were weighed, then incubated in 150 µl of the feeding buffer containing C^{14}-*tZ* or -SAM as described above. After 1 h incubation, the feeding solution was removed and the leaves were washed three times with 1 ml 5 mM MES-KOH (pH 5.6) buffer. For our time–course experiments, the fed leaves were sampled after an incubation of 5, 15, 30, 45 or 60 min. For sodium vanadate treatment, the sampled leaves were pre-treated in 150 µl 5 mM MES-KOH (pH 5.6) buffer with 1 mM sodium vanadata for 30 min, then the buffer was replaced with 150 µl 5 mM MES-KOH (pH 5.6) buffer containing 1 mM sodium vanadata and 5 nM C^{14}-*tZ* and incubated for 1 h. After collecting and washing, the leaf samples were mixed with 200 µl bleach and incubated at 55 °C for 2 h to solubilize the tissue. Radioactivity was quantified by a scintillation counter.

References

1. Sakakibara, H. Cytokinins: activity, biosynthesis, and translocation. *Annu. Rev. Plant Biol.* **57,** 431–449 (2006).
2. Moubayidin, L., Di Mambro, R. & Sabatini, S. Cytokinin-auxin crosstalk. *Trends Plant Sci.* **14,** 557–562 (2009).
3. Ha, S. et al. Cytokinins: metabolism and function in plant adaptation to environmental stresses. *Trends Plant Sci.* **17,** 172–179 (2012).
4. Matsumoto-Kitano, M. et al. Cytokinins are central regulators of cambial activity. *Proc. Natl Acad. Sci. USA* **105,** 20027–20031 (2008).
5. Chory, J. et al. A role for cytokinins in de-etiolation in Arabidopsis (det mutants have an altered response to cytokinins). *Plant Physiol.* **104,** 339–347 (1994).
6. Gan, S. & Amasino, R. M. Inhibition of leaf senescence by autoregulated production of cytokinin. *Science* **270,** 1986–1988 (1995).
7. Davies, C. R., Seth, A. K. & Wareing, P. F. Auxin and kinetin interaction in apical dominance. *Science* **151,** 468–469 (1966).
8. Werner, T. et al. Root-specific reduction of cytokinin causes enhanced root growth, drought tolerance, and leaf mineral enrichment in Arabidopsis and tobacco. *Plant Cell* **22,** 3905–3920 (2010).
9. Hwang, I., Sheen, J. & Muller, B. Cytokinin signaling networks. *Annu. Rev. Plant Biol.* **63,** 353–380 (2012).
10. Hirose, N. et al. Regulation of cytokinin biosynthesis, compartmentalization and translocation. *J. Exp. Bot.* **59,** 75–83 (2008).
11. Burkle, L. et al. Transport of cytokinins mediated by purine transporters of the PUP family expressed in phloem, hydathodes, and pollen of Arabidopsis. *Plant J.* **34,** 13–26 (2003).
12. Gillissen, B. et al. A new family of high-affinity transporters for adenine, cytosine, and purine derivatives in Arabidopsis. *Plant Cell* **12,** 291–300 (2000).
13. Hirose, N., Makita, N., Yamaya, T. & Sakakibara, H. Functional characterization and expression analysis of a gene, OsENT2, encoding an equilibrative nucleoside transporter in rice suggest a function in cytokinin transport. *Plant Physiol.* **138,** 196–206 (2005).
14. Sun, J. et al. Arabidopsis SOI33/AtENT8 gene encodes a putative equilibrative nucleoside transporter that is involved in cytokinin transport in planta. *J. Integr. Plant Biol.* **47,** 588–603 (2005).
15. Kudo, T., Kiba, T. & Sakakibara, H. Metabolism and long-distance translocation of cytokinins. *J. Integr. Plant Biol.* **52,** 53–60 (2010).
16. Verrier, P. J. et al. Plant ABC proteins—a unified nomenclature and updated inventory. *Trends Plant Sci.* **13,** 151–159 (2008).
17. Rea, P. A. Plant ATP-binding cassette transporters. *Annu. Rev. Plant Biol.* **58,** 347–375 (2007).
18. Pighin, J. A. et al. Plant cuticular lipid export requires an ABC transporter. *Science* **306,** 702–704 (2004).
19. Kuromori, T. et al. ABC transporter AtABCG25 is involved in abscisic acid transport and responses. *Proc. Natl Acad. Sci. USA* **107,** 2361–2366 (2010).
20. Ruzicka, K. et al. Arabidopsis PIS1 encodes the ABCG37 transporter of auxinic compounds including the auxin precursor indole-3-butyric acid. *Proc. Natl Acad. Sci. USA* **107,** 10749–10753 (2010).
21. Riefler, M., Novak, O., Strnad, M. & Schmulling, T. Arabidopsis cytokinin receptor mutants reveal functions in shoot growth, leaf senescence, seed size, germination, root development, and cytokinin metabolism. *Plant Cell* **18,** 40–54 (2006).
22. Werner, T. et al. Cytokinin-deficient transgenic Arabidopsis plants show multiple developmental alterations indicating opposite functions of cytokinins in the regulation of shoot and root meristem activity. *Plant Cell* **15,** 2532–2550 (2003).
23. Higuchi, M. et al. In planta functions of the Arabidopsis cytokinin receptor family. *Proc. Natl Acad. Sci. USA* **101,** 8821–8826 (2004).
24. Ruzicka, K. et al. Cytokinin regulates root meristem activity via modulation of the polar auxin transport. *Proc. Natl Acad. Sci. USA* **106,** 4284–4289 (2009).
25. Colon-Carmona, A., You, R., Haimovitch-Gal, T. & Doerner, P. Technical advance: spatio-temporal analysis of mitotic activity with a labile cyclin-GUS fusion protein. *Plant J.* **20,** 503–508 (1999).
26. Werner, T., Motyka, V., Strnad, M. & Schmulling, T. Regulation of plant growth by cytokinin. *Proc. Natl Acad. Sci. USA* **98,** 10487–10492 (2001).
27. D'Agostino, I. B., Deruere, J. & Kieber, J. J. Characterization of the response of the Arabidopsis response regulator gene family to cytokinin. *Plant Physiol.* **124,** 1706–1717 (2000).
28. Svacinova, J. et al. A new approach for cytokinin isolation from Arabidopsis tissues using miniaturized purification: pipette tip solid-phase extraction. *Plant Methods* **8,** 17 (2012).
29. Dello Ioio, R. et al. A genetic framework for the control of cell division and differentiation in the root meristem. *Science* **322,** 1380–1384 (2008).
30. Kang, J. et al. Plant ABC transporters. *Arabidopsis Book* **9,** e0153 (2011).
31. McFarlane, H. E., Shin, J. J., Bird, D. A. & Samuels, A. L. Arabidopsis ABCG transporters, which are required for export of diverse cuticular lipids, dimerize in different combinations. *Plant Cell* **22,** 3066–3075 (2010).
32. Larsson, C., Sommarin, M. & Widell, S. Isolation of highly purified plant plasma membranes and separation of inside-out and right-side-out vesicles. *Methods Enzymol.* **228,** 451–469 (1994).
33. Takei, K. et al. AtIPT3 is a key determinant of nitrate-dependent cytokinin biosynthesis in Arabidopsis. *Plant Cell Physiol.* **45,** 1053–1062 (2004).
34. Kuroha, T. et al. A trans-zeatin riboside in root xylem sap negatively regulates adventitious root formation on cucumber hypocotyls. *J. Exp. Bot.* **53,** 2193–2200 (2002).
35. Takano, J. et al. Arabidopsis boron transporter for xylem loading. *Nature* **420,** 337–340 (2002).
36. Inoue, T. et al. Identification of CRE1 as a cytokinin receptor from Arabidopsis. *Nature* **409,** 1060–1063 (2001).
37. Ashikari, M. et al. Cytokinin oxidase regulates rice grain production. *Science* **309,** 741–745 (2005).

38. Bartrina, I. *et al.* Cytokinin regulates the activity of reproductive meristems, flower organ size, ovule formation, and thus seed yield in Arabidopsis thaliana. *Plant Cell* **23,** 69–80 (2011).

39. Spiess, L. D. Comparative activity of isomers of zeatin and ribosyl-zeatin on Funaria hygrometrica. *Plant Physiol.* **55,** 583–585 (1975).

40. Zhang, K. W. *et al.* An engineered monolignol 4-*O*-methyltransferase (MOMT4) represses lignin polymerization and confers novel metabolic capability in Arabidopsis. *Plant Cell* **24,** 3122–3139 (2012).

41. Tzfira, T. *et al.* pSAT vectors: a modular series of plasmids for autofluorescent protein tagging and expression of multiple genes in plants. *Plant Mol. Biol.* **57,** 503–516 (2005).

42. Yoo, S. D., Cho, Y. H. & Sheen, J. Arabidopsis mesophyll protoplasts: a versatile cell system for transient gene expression analysis. *Nat. Protoc.* **2,** 1565–1572 (2007).

43. Miao, Y. C. & Liu, C. J. ATP-binding cassette-like transporters are involved in the transport of lignin precursors across plasma and vacuolar membranes. *Proc. Natl Acad. Sci. USA* **107,** 22728–22733 (2010).

44. Jefferson, R. A., Kavanagh, T. A. & Bevan, M. W. GUS fusions: beta-glucuronidase as a sensitive and versatile gene fusion marker in higher plants. *EMBO J.* **6,** 3901–3907 (1987).

Author contributions

K.Z. and C.-J.L. designed the research; K.Z., G.M., Z.W., H.Y., Y.C. and X.Z. conducted most experiments; O.N. performed cytokinin profiling; Y.Y. attempted *in vitro* functional assessments; K.Z., M.S. and C.-J.L. analysed data; K.Z. and C.-J.L. wrote the paper. All authors discussed the results and collectively edited the manuscript.

Additional information

Accession numbers: Sequence data have been deposited in the GenBank/European Molecular Biology Laboratory databases under the following accession codes: AT1G31770 (*AtABCG14*), AT3G18780 (*ACTIN 2*), At4G05320 (*UBIQUITIN 10*), AT3G48100 (*ARR5*), AT4G37490 (*CYCB1;1*).

Supplementary Information accompanies this paper at http://www.nature.com/naturecommunications

Competing financial interests: The authors declare no competing financial interests.

Reprints and permission information is available online at http://npg.nature.com/reprintsandpermissions/

How to cite this article: Zhang, K. *et al. Arabidopsis* ABCG14 protein controls the acropetal translocation of root-synthesized cytokinins. *Nat. Commun.* 5:3274 doi: 10.1038/ncomms4274 (2014).